

Frustration in an exactly solvable mixed-spin Ising model with bilinear and three-site four-spin interactions on a decorated square lattice [☆]

M. Jaščur^{a,*}, V. Štubňa^a, K. Szałowski^b, T. Balcerzak^b

^a*Department of Theoretical Physics and Astrophysics, Institute of Physics, P.J. Šafárik University in Košice, Park Angelinum 9, 040 01 Košice, Slovakia*

^b*Department of Solid State Physics, Faculty of Physics and Applied Informatics, University of Łódź, ul. Pomorska 149/153, 90-236 Łódź, Poland*

Abstract

Competitive effects of so-called three-site four-spin interactions, single ion anisotropy and bilinear interactions is studied in the mixed spin-1/2 and spin-1 Ising model on a decorated square lattice. Exploring the decoration-iteration transformation, we have obtained exact closed-form expressions for the partition function and other thermodynamic quantities of the model. From these relations, we have numerically determined ground-state and finite-temperature phase diagrams of the system. We have also investigated temperature variations of the correlation functions, internal energy, entropy, specific heat and Helmholtz free energy of the system. From the physical point of view, the most interesting result represents our observation of a partially ordered ferromagnetic or phase in the system with zero bilinear interactions. It is remarkable, that due to strong frustrations disordered spins survive in the system even at zero temperature, so that the ground state of the system becomes macroscopically degenerate with non-zero entropy. Introduction of arbitrarily small bilinear interaction completely removes degeneracy and the entropy always goes to zero at the the ground state.

Keywords: frustration, Ising model, many-body interactions, exact results, decorated lattice, phase transitions.

1. Introduction

The investigation of multi-spin interactions has been initiated several decades ago in order to clarify their influence on phase transitions and magnetic properties in various physical systems. In order to investigate basic aspects of multi-spin interactions the authors have utilized various theoretical methods including exact calculations [1]-[15], series

[☆]This work has been supported under grant VEGA No. 1/0234/14 and APVV-14-0073

*Corresponding author

Email addresses: michal.jascur@upjs.sk (M. Jaščur), viliamstubna@yahoo.com (V. Štubňa), kszalowski@uni.lodz.pl (K. Szałowski), tadeusz.balcerzak@gmail.com (T. Balcerzak)

expansions [16]-[18], renormalization-group techniques [19]-[22], Monte Carlo simulations [23]-[26], mean-field and effective-field theory [27]-[30].

On the other hand, from the experimental point of view, the models with multi-spin interactions have been widely used to explain the thermodynamic properties of various physical systems, such as binary alloys [23], classical fluids [31], solid He₃ [32], lipid bilayers [33], metamagnets [34], rare gases [35] or hydrogen bonded ferroelectrics PbHPO₄ and PbDPO₄ [36]. One should also mention here that the models with multi-spin interactions have been successfully used to describe the first-order phase transition in the squaric acid crystal H₂C₂O₄ [27, 37, 38] and some co-polymers [39]. Moreover, the cycling four-spin exchange interactions have been adopted to explain experimental results on spin gaps [40]-[42], Raman peaks [43] and optical conductivity of the cuprate ladder La₂Ca_{14-x}Cu₂₄O₄₁ [44]. The four-spin interactions have been taken into account also in the study of two-dimensional antiferromagnet La₂CuO₄, the parent material of high-T_c superconductors [45, 46]. A special kind of higher-order spin interactions that are known as three-site four-spin ones has been introduced and widely studied Iwashita and Uryu [47]-[50]. Finally, let us mention a series of works by Köbler et al. [51]-[54] in which the authors have very carefully investigated the role of higher-order spin interactions in a wide class of real magnetic materials.

As far as it concerns of magnetic properties, the models with multi-spin interactions may exhibit some peculiarities, for example, the non-universal critical behavior [1, 2, 17, 18] or deviations from the Bloch's T^{3/2} law at low temperatures [51]-[54]. Here it is worth emphasizing that some of these phenomena are not yet well understood and clarified even at the present time. In fact, the investigation of many-body interactions is of tremendous importance in all branches of physics, since such studies may discover new physical phenomena that do not appear in the systems with pair interactions only. However, it is necessary to recall that the investigation of the systems with many-body interactions is as a rule much more complex than those with pair interactions only. Nonetheless, we have recently demonstrated [11]-[15] that various versions of the Ising model represent a very good theoretical ground for an accurate treatment of multi-spin interactions.

The main aim of this work is to extend our recent research in this field in order to investigate in detail the role of so-called three-site four-spin interactions in crystalline systems with localized magnetic moments. For this purpose, we will study the mixed-spin 1/2 and 1 Ising model with the single-ion anisotropy, pair and three-site four spin interactions on a decorated square lattice. The outline of the present work is as follows. In Sec. 2 and 3 we derive exact equations for all physical quantities applying a generalized form of decoration-iteration transformation. The ground-state and finite-temperature phase diagrams are discussed in detail in Sec. 4 along with thermal variations of other physical quantities. Finally some conclusions are sketched in the last section.

2. Theory

In this work we will investigate the mixed spin-1/2 and spin-1 Ising model on a decorated square lattice depicted in Fig. 1. The system is described by the Hamiltonian

$$\mathcal{H} = -\frac{J}{2} \sum_{i,j} \mu_i^z S_j^z - \frac{J'}{2} \sum_{i,j} \mu_i^z \mu_j^z - J_4 \sum_k \mu_{k1}^z (S_k^z)^2 \mu_{k2}^z - D \sum_k (S_k^z)^2 \quad (1)$$

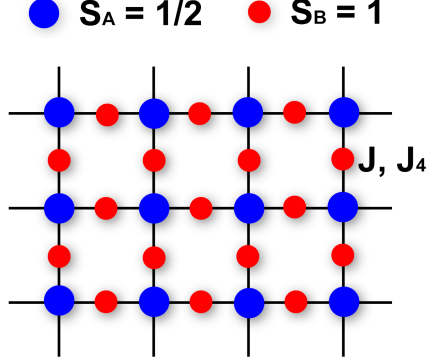


Figure 1: Part of a mixed spin decorated square lattice. Blue circles located on the original square lattice nodes denote the spin-1/2 atoms and the red ones represent decorating atoms with spin 1 located at each bond of the square lattice.

where J and J' respectively denote the nearest-neighbor and next-nearest-neighbor bilinear exchange interactions, J_4 is the three-site four-spin exchange interaction and D represents the single-ion anisotropy parameter. The summations in the first and second term in (1) run over all relevant pairs on the decorated square lattice, while in the third and fourth term the summations are over all decorating spins, i.e. $k = 1, \dots, 2N$, where N represents the total number of spin-1/2 atoms.

In order to apply the decoration-iteration transformation to the present model, we at first express the total Hamiltonian in the form

$$\mathcal{H} = \sum_k \mathcal{H}_k, \quad (2)$$

where the Hamiltonian \mathcal{H}_k includes all interaction terms within the k -th bond of the lattice and it is given by

$$\mathcal{H}_k = -J(\mu_{ki}^z + \mu_{kj}^z)S_k^z - J'\mu_{ki}^z\mu_{kj}^z - J_4\mu_{ki}^z\mu_{kj}^z(S_k^z)^2 - D(S_k^z)^2 \quad (3)$$

Now, using (2), the partition function of the model can be expressed as

$$\mathcal{Z} = \sum_{\{\mu_{k\gamma}^z = \pm 1/2\}} \sum_{\{S_k^z = \pm 1, 0\}} \exp(-\beta\mathcal{H}) = \sum_{\{\mu_{k\gamma}^z = \pm 1/2\}} \prod_{k=1}^{2N} \sum_{S_k^z = \pm 1, 0} \exp(-\beta\mathcal{H}_k), \quad (4)$$

where the curled brackets denote the fact that relevant summation concerns all spin variables of the lattice.

Introducing the following decoration-iteration transformation [55, 56, 57]

$$\sum_{S_k^z = \pm 1, 0} \exp(-\beta\mathcal{H}_k) = A \exp(\beta\mu_{ki}^z\mu_{kj}^z) \quad (5)$$

one rewrites equation (4) as follows

$$\mathcal{Z} = A^{2N} \mathcal{Z}_0(\beta R). \quad (6)$$

In the last equation $\mathcal{Z}_0(\beta R)$ represents the partition function of conventional Ising model on a square lattice described by the Hamiltonian $\mathcal{H}_0 = -R \sum_k \mu_{ki}^z \mu_{kj}^z$. This partition function has been exactly calculated in a seminal Onsager's work [58] and it will be used in this paper to obtain exact results for thermodynamic properties of the model under investigation. Of course, to complete the calculation of \mathcal{Z} we have also to determine the unknown functions A and R . Fortunately, this evaluation may be straightforwardly performed by substituting $\mu_{ki}^z = \pm 1/2$ and $\mu_{kj}^z = \pm 1/2$ into Eq. (5) and in this way one gets

$$A = \sqrt{w_1 w_2}, \quad \beta R = \beta J' + 2 \ln \left(\frac{w_1}{w_2} \right), \quad (7)$$

where

$$w_1 = 1 + 2e^{\beta D + \frac{\beta J_A}{4}} \cosh(\beta J) \quad (8)$$

$$w_2 = 1 + 2e^{\beta D - \frac{\beta J_A}{4}}. \quad (9)$$

3. Ground-state and thermodynamic properties

The ground-state phase diagram can be determined investigating the internal energy of the system at $T = 0$. Since we do not consider any external field, the internal energy of the system can be evaluated as a mean value of the Hamiltonian (1), i.e. $U = \langle \mathcal{H} \rangle$ and it takes the following form

$$\frac{U}{2N} = -J \langle (\mu_{k1}^z + \mu_{k2}^z) S_k^z \rangle - J' \langle \mu_{k1}^z \mu_{k2}^z \rangle - J_4 \langle \mu_{k1}^z (S_k^z)^2 \mu_{k2}^z \rangle - D \langle (S_k^z)^2 \rangle, \quad (10)$$

where the angular brackets denote the standard canonical averaging using the density matrix $\rho = \exp(-\beta \mathcal{H}) / \mathcal{Z}$. For further progress in calculation it is of crucial importance that all correlation functions entering previous equation can be calculated using the generalized Callen-Suzuki identities [59, 60] which in our case take the form

$$\langle S_j^z f_k \rangle = \left\langle f_k \frac{2e^{\beta J_4 \mu_{ki}^z \mu_{kj}^z} \sinh[\beta J (\mu_{ki}^z + \mu_{kj}^z)]}{2e^{\beta J_4 \mu_{ki}^z \mu_{kj}^z} \cosh[\beta J (\mu_{ki}^z + \mu_{kj}^z)] + e^{-\beta D}} \right\rangle, \quad (11)$$

$$\langle (S_k^z)^2 f_k \rangle = \left\langle f_k \frac{2e^{\beta J_4 \mu_{ki}^z \mu_{kj}^z} \cosh[\beta J (\mu_{ki}^z + \mu_{kj}^z)]}{2e^{\beta J_4 \mu_{ki}^z \mu_{kj}^z} \cosh[\beta J (\mu_{ki}^z + \mu_{kj}^z)] + e^{-\beta D}} \right\rangle, \quad (12)$$

where f_k represents a function of arbitrary spin variables except of the variable S_k^z .

Now applying the well-known differential operator technique [61], we recast previous equation in the more convenient form

$$\langle S_k^z f_k \rangle = \langle f_k(\mu_{ki}^z + \mu_{kj}^z) \rangle A_1 \quad (13)$$

and

$$\langle (S_k^z)^2 f_k \rangle = \langle f_k \rangle A_0 + 4 \langle f_k \mu_{ki}^z \mu_{kj}^z \rangle A_2, \quad (14)$$

where the coefficients $A_i = A_i(\beta, J, J_4, D)$ are listed in the Appendix.

It is clear that after substituting $f_k = 1$ into Eq. (13) and Eq. (14), we respectively obtain equations for the evaluation of sublattice magnetization $m_B = \langle S_k^z \rangle$ and quadrupolar moment $q_B = \langle (S_k^z)^2 \rangle$. Similarly, setting $f_k = (\mu_{ki}^z + \mu_{kj}^z)$ one gets expressions for the correlation functions $\langle S_k^z (\mu_{ki}^z + \mu_{kj}^z) \rangle$ and $\langle \mu_{ki}^z (S_k^z)^2 \mu_{kj}^z \rangle$, that are necessary for evaluation of the internal energy according to (10). Finally, it is also very important to notice that the magnetization of nodal spins $m_A = \langle \mu_{ki}^z \rangle = \langle \mu_{kj}^z \rangle$ and also the correlation function $c = \langle \mu_{ki}^z \mu_{kj}^z \rangle$ appearing on the r.h.s of (13) and (14) can be simply evaluated from the relations

$$m_A = \langle \mu_{ki}^z \rangle = \langle \mu_{kj}^z \rangle = \langle \mu_{ki}^z \rangle_0 = \langle \mu_{kj}^z \rangle_0 = m_0 \quad (15)$$

and

$$c = \langle \mu_{ki}^z \mu_{kj}^z \rangle = \langle \mu_{ki}^z \mu_{kj}^z \rangle_0 = c_0, \quad (16)$$

where the $\langle \dots \rangle_0$ represents relevant canonical averaging on the original (non-decorated) square lattice using the density matrix $\rho_0 = \exp(-\beta \mathcal{H}_0) / \mathcal{Z}_0$.

Calculation of other thermodynamic quantities is a straightforward process, since in the previous section we have obtained an exact relation for the partition function of the model under investigation (see Eqs (6)-(9)).

At first, the Helmholtz free energy is easily obtained in the form

$$F(J, J_4, J', D) = -2N\beta^{-1} \ln A(J, J_4, J', D) + F_0(\beta, R), \quad (17)$$

where parameters A, R are given by Eq. (7) and $F_0(\beta, R)$ represents the Helmholtz free energy of the Ising square lattice [58]

$$F_0(\beta, R) = -\frac{4N}{\beta} \ln \left(\cosh \frac{\beta R}{2} \right) - \frac{4N}{\beta} \frac{1}{2\pi} \int_0^\pi \ln \left[\frac{1}{2} \left(1 + \sqrt{1 - \kappa^2 \sin^2 \phi} \right) \right] d\phi \quad (18)$$

with

$$\kappa = \frac{2 \sinh \left(\frac{\beta R}{2} \right)}{\cosh^2 \left(\frac{\beta R}{2} \right)}. \quad (19)$$

It is clear that the contribution from decorating spins to the total Helmholtz free energy is represented by the first term in Eq. (17) which is an analytic function in the whole parameter space. Therefore the critical behavior of the model will necessarily belong to the same universality class as that one of the usual 2D Ising model. Consequently, the finite-temperature phase boundaries of the system under investigation can be simply determined by substituting the inverse critical temperature of the square lattice $\beta_c R = 2 \ln(\sqrt{2} + 1)$ into Eq. (7), i.e.

$$2 \ln(\sqrt{2} + 1) = \beta_c J' + 2 \ln \frac{1 + 2 \exp(\beta_c D + \frac{\beta_c J_4}{4}) \cosh(\beta_c J)}{1 + 2 \exp(\beta_c D - \frac{\beta_c J_4}{4})}, \quad (20)$$

with $\beta_c = 1/(k_B T_c)$.

In this work we will also study the entropy and specific heat that are respectively given by the relations

$$S = \frac{U - F}{T} \quad (21)$$

and

$$C_0 = \left(\frac{\partial U}{\partial T} \right)_0. \quad (22)$$

Here the subscript zero indicates the fact that relevant quantity is calculated in the zero external magnetic field.

Numerical results obtained from the above equations are discussed in detail in the next section.

4. Numerical results

In this section we will discuss the most interesting numerical results for the ground-state and finite-temperature phase diagrams, and thermal dependencies of magnetization, correlation functions, internal energy, entropy and specific heat. For this purpose it is useful to introduce the following dimensionless parameters: $\alpha = J/J_4$, $\lambda = J'/J_4$ and $d = D/J_4$.

4.1. Ground-state phase diagram

In order to investigate the physical nature of possible phases at the ground state, we have numerically studied the sublattice magnetizations, quadrupolar moment and various correlations functions in our system at $T = 0$. On the basis of these calculations, the ground-state phase boundaries have been established from the minimum values of the internal energy of the system. Our results are summarized in Fig. 2, where we have depicted the ground-state phase diagram in the $\alpha - d$ space for the special case of $\lambda = 0$, i.e. $J' = 0$. As one can see from the figure, the ordered ferrimagnetic phase becomes stable in the region above the line $d = \alpha - 0.25$ for negative values of nearest-neighbor pair exchange interaction ($\alpha < 0$). On the other hand, for $\alpha > 0$ the ferromagnetic ordering appears in the region above the line $d = -\alpha - 0.25$. It also clear that for $d > -0.25$ the ordered ferrimagnetic or ferromagnetic phase is respectively stable for arbitrary negative or positive nonzero values of α . Next, it follows from our analysis that

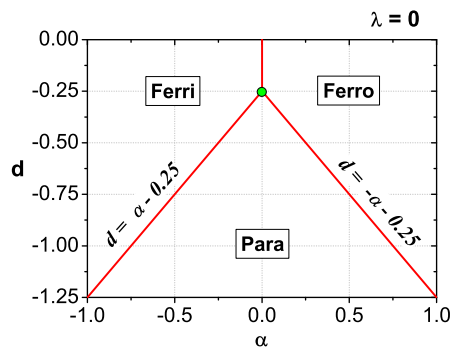


Figure 2: Ground-state phase diagram in the $\alpha - d$ space for the mixed-spin Ising model without next-nearest pair interaction ($\lambda = 0$).

a disordered paramagnetic phase becomes stable in the ground state for arbitrary values

of α whenever the crystal-field parameter d satisfies inequality $d < -|\alpha| - 0.25$, i.e. when the single-ion anisotropy takes negative and strong enough values. Consequently, the ordered phases coexist with the paramagnetic one along the line $d = -|\alpha| - 0.25$ and the system exhibits a first-order phase transition when crossing this line.

Now, let us look closely at the particular case of system with pure three-site interaction which is obtained by setting $\alpha = \lambda = 0$. In this case one finds from Eq. (13) that the sublattice magnetization m_B becomes zero for arbitrary values of d and of course, the same statement applies also for all correlations including a spin of B sublattice. Moreover, one finds from Eq. (14) that $\langle (S_k^z)^2 \rangle = 1$ for $d > -0.25$, thus the spin states $S_k^z = +1$ and $S_k^z = -1$ of all decorating atoms are equally likely occupied at $T = 0$, while the sublattice A exhibits the long-range order with $m_A = 1/2$. Thus the system as a whole exhibits an unexpected behavior with the non-zero ground-state entropy $S_0/N = k_B \ln 4 \doteq 1.386k_B$ belonging to the partially ordered magnetic phase. This surprising behavior appears as a result of the interplay between three-site four-spin interaction J_4 and crystal-field parameter D . On the other hand, for $\alpha = 0$ and $d < -0.25$ we obtain from Eq. (14) $\langle (S_k^z)^2 \rangle = 0$ indicating that all decorating atoms occupy the spin states $S_k^z = 0$, so that each atom on the A sublattice is surrounded by decorating atoms with $S_k^z = 0$. As a result of this spin configuration, each atom of the A sublattice can be found equally likely in the spin state $\mu_{k,j}^z = +1/2$ or $\mu_{k,j}^z = -1/2$ thus the entropy at $T = 0$ takes now the value $S_0/N = k_B \ln 2 \doteq 0.693k_B$. In this case, of course, no magnetic order appears in the ground state.

Moreover, one should emphasize here that at the point with co-ordinates $\alpha = 0$ and $d = -0.25$ one observes a very interesting partially ordered phase with $m_B = 0$, $\langle (S_k^z)^2 \rangle \doteq 0.642$, nonzero $m_A \doteq 0.476$ and unusually high entropy $S_0/N \doteq 2.213k_B$ at $T = 0$. As far as we know, such a phase has not been reported in the literature on the Ising model until now.

In order to complete the ground-state analysis, let us briefly mention the effect of a positive next-nearest-neighbor interaction, i.e. $\lambda > 0$. It is clear that in this case the disordered paramagnetic phase never becomes stable for $\alpha \neq 0$ at $T = 0$, so that the system will always exhibit the long-range order with $(m_A, m_B) = (1/2, 1)$ for $\alpha > 0$, and $(m_A, m_B) = (1/2, -1)$ for $\alpha < 0$. On the other hand, the situation for $\alpha = 0$, $d > -0.25$ and $\lambda > 0$ becomes identical with the above discussed case with $\alpha = 0$, $d > -0.25$ and $\lambda = 0$. Finally, for $\alpha = 0$, $d < -0.25$ and $\lambda > 0$, the system will exhibit a long-range order on the A sublattice, despite of the fact that all atoms of the B sublattice will occupy the zero-spin states. However, contrary to the case with $\lambda = 0$, the entropy of the system now always vanishes in the limit of $T \rightarrow 0$.

4.2. Phase diagrams and compensation temperatures

Now, let us proceed with the discussion of finite-temperature phase diagrams and compensation temperatures. We recall that the critical temperature is calculated from Eq. (20) and takes the same value for both ferromagnetic and ferrimagnetic cases. In ferrimagnetic systems, the compensation temperature is defined as a temperature at which the total magnetization vanishes below the critical temperature, so that in our case it is determined by the condition $m = (m_A + 2m_B) = 0$. In what follows, we will discuss the most interesting results of phase diagrams and compensation temperatures obtained numerically for some characteristic combinations of freely adjustable parameters.

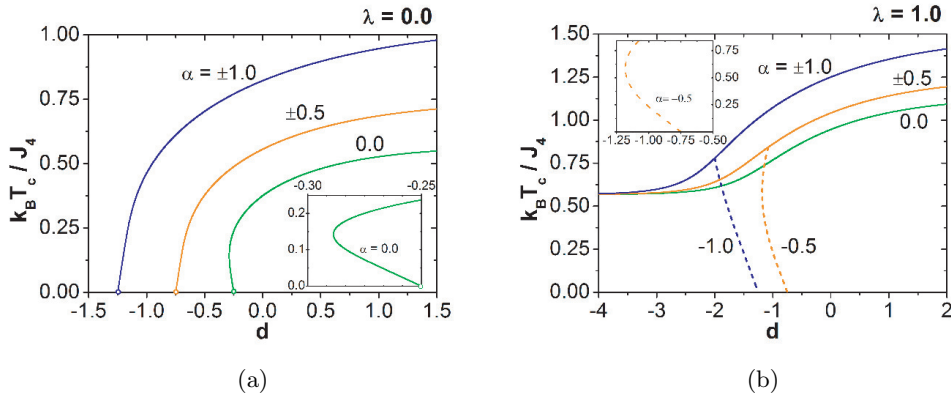


Figure 3: (a) - Phase diagrams of the decorated mixed-spin Ising system in the $d - T_c$ space for $\lambda = 0$ and for several typical values of α . The inset shows the detail view for $\alpha = 0.0$ where the reentrant behavior with two critical temperatures appears. (b) - The same as in the case (a) but for $\lambda = 1.0$. The critical boundaries are depicted by full lines and compensation temperatures by dashed ones. The inset shows the existence of two compensation temperatures in a narrow region of negative values of d .

At first, in Fig. 3a there are depicted the dependencies of critical temperatures on the reduced single-ion anisotropy parameter d for $|\alpha| = 0, 0.5$ and 1 . As we can see from the figure, the phase boundaries for arbitrary $\alpha \neq 0$ do not depend on the sign of the nearest-neighbor interaction, so that both the ferromagnetic ($m_A > 0, m_B > 0$) and ferrimagnetic ($m_A > 0, m_B < 0$) phases always vanish at the same critical temperature. This statement follows, of course, directly from Eq. (20) which is invariant under changing the sign of J . In agreement with our discussion in previous section, one finds that magnetization of the system for both ordered phases takes its saturation value at $T = 0$ in the region of $d > -|\alpha| - 0.25$. Of course, by increasing the temperature, the magnetization will gradually decrease until it continuously vanishes at some critical temperature T_c above which the disordered paramagnetic phase becomes stable. Moreover, as we have already mentioned above, the relevant second-order phase transitions belong to the 2D Ising universality class. Next, one also observes from Fig. 3a that the region of stability of paramagnetic phase extends from high temperatures down to zero absolute temperature for arbitrary values of parameter α , whenever $d < -|\alpha| - 0.25$. Here one should also notice that if $\lambda = 0$ then no compensation points appear in the system, regardless of the values of parameters α and d . Now, let us inspect the special case of the system with the pure three-site four-spin interaction, i.e. $\alpha = 0$ and $\lambda = 0$. In this case one finds that for $d > -0.25$, the partially ordered phase with $m_A \neq 0$ and $m_B = 0$ is stable below T_c , while above the critical temperature becomes stable again the standard paramagnetic phase. Moreover, looking carefully on the phase boundary one finds the C-shaped form of this curve indicating the appearance of reentrant behavior with two phase transitions in a narrow low-temperature region in the neighborhood of $d = -0.25$ (see the inset in Fig. 3a). As we have already mentioned earlier, the non-zero next-nearest-neighbor pair interaction ($\lambda \neq 0$) eliminates the existence of paramagnetic phase

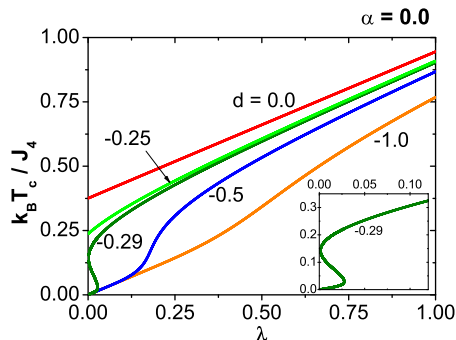


Figure 4: Phase diagrams of the decorated mixed-spin Ising system in the $\lambda - T_c$ space for $\alpha = 0$ and for several typical values of d . The inset shows the detail view for $d = -0.29$ where the reentrant behavior with three critical temperatures appears.

at $T = 0$, regardless of the values of other parameters, so that the phase boundaries must significantly change. For $\lambda = 1.0$ and for the same values of α as in Fig. 3a, the situation is illustrated in Fig. 3b where we have depicted using full lines some typical phase boundaries. Regarding the compensation temperatures one should stress here that,

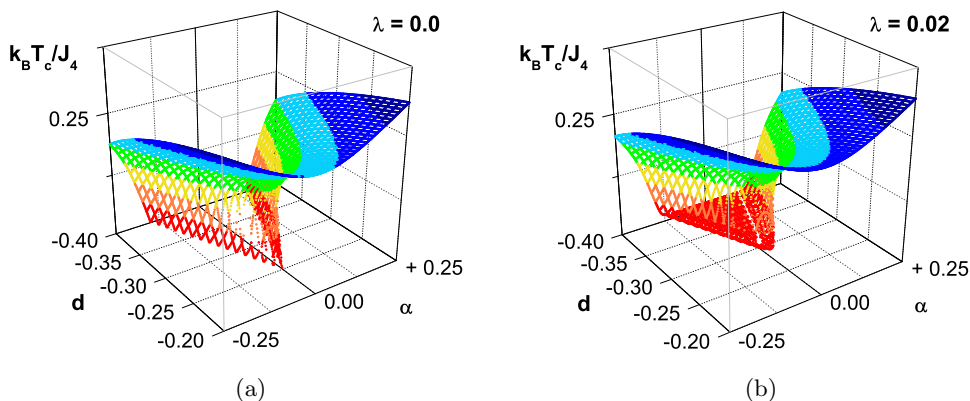


Figure 5: Global phase diagrams of the decorated mixed-spin Ising system in the $d - \alpha - T_c$ space for $\lambda = 0$ (a) and $\lambda = 0.02$ (b), that is without and with the small next-nearest-neighbor interaction, respectively.

in general, the compensation effect is only possible for relatively strong nonzero values of λ , which keeps the sublattice magnetization m_A strong enough over a large temperature region. The typical dependencies of the compensation temperature on the parameter d are shown in Fig. 3b by dashed lines for $\lambda = 1.0$, $\alpha = -1.0$ and $\alpha = -0.5$. The inset in this figure illustrates that even two compensation temperatures are possible in a narrow region of negative values of d . As far as we know, such a finding has not been reported yet for the systems with higher order interactions.

Moreover, a closer investigation of the particular case with $\alpha = 0$ and $\lambda \neq 0$ indicates

that the re-entrant behavior with three different critical temperatures appears in the neighborhood of $d \approx -0.3$. This phenomenon is most clearly visible when the phase diagrams are constructed in the $\lambda - T_c$ space as it is shown in Fig. 4.

Finally, to in order to obtain a global view of the critical surface, we have combined together different two dimensional phase diagrams and we have obtained the three-dimensional global phase diagrams of the system that are presented in Figs. 5a and 5b for $\lambda = 0$ and $\lambda = 0.02$, respectively.

4.3. Magnetization, entropy and specific heat

In this part we present the most interesting numerical results for thermal dependencies of thermodynamic quantities. In order to demonstrate the role of the three-site four-spin interaction, we at first in Figs. 6a and 6b show the temperature dependencies of sublattice magnetization and quadrupolar moment q_B for $\alpha = \lambda = 0$ and for several representative values of d . Let us recall that the sublattice B does not exhibit the long-range order, since the magnetization m_B vanishes for arbitrary values of d and at any temperature, whenever $\alpha = 0$ holds. Consequently, at $T = 0$ the system as a whole will be partially

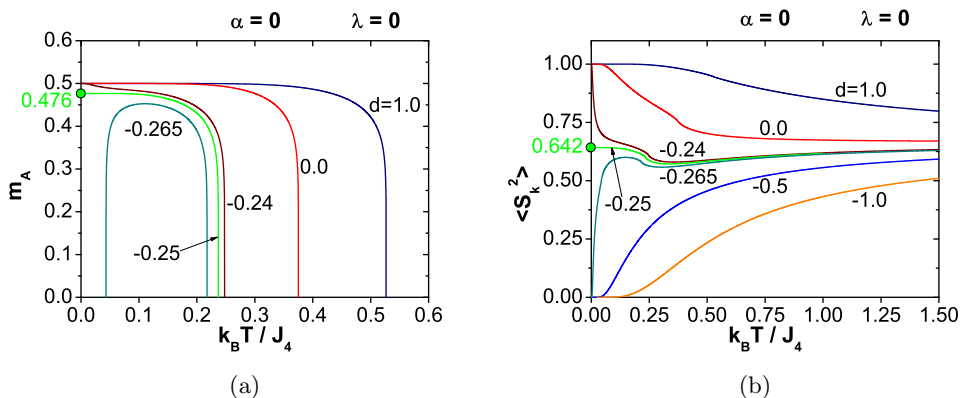


Figure 6: Thermal dependencies of sublattice magnetization m_A and quadrupolar momentum $\langle (S_k^z)^2 \rangle$ of the decorated mixed-spin Ising system for $\alpha = \lambda = 0$ and for several typical values of d .

ferromagnetically ordered for $d > -0.25$ with $m_A = 0.5$, $m_B = 0$ and $q_B = 1$ as it is clearly illustrated in Figs. 6a and 6b for $d = -0.24, 0$ and 1.0 . Moreover, at the ground state for $\alpha = \lambda = 0$ and $d = -0.25$ one finds that the sublattice magnetization takes the value $m_A = 0.476$ and the quadrupolar moment $q_B = 0.642$, instead of their saturation values 0.5 and 1 , respectively. These values indicate that both sublattices exhibit very interesting frustrated behavior which originates from the effect of the three-site four-spin interaction and, as far as we know, such a finding has not been reported for the Ising models until now. Finally, selecting the value of d slightly below $d = -0.25$ one observes a reentrant behavior in the temperature behavior of the magnetization m_A as it is shown in Fig. 6a for $d = -0.265$. Of course, one can very simply verify that all thermal dependencies are in a perfect agreement with the ground-state and finite-temperature phase diagrams discussed in previous section, since $m_A = m_B = q_B = 0$ at $T = 0$.

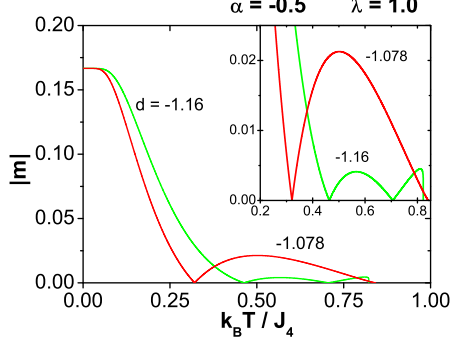


Figure 7: Temperature dependencies of the absolute value of total reduced magnetization $|m| = |m_A + 2m_M|/3N$. The parameters of the model are fixed to the selected specific values in order to illustrate the cases with one and two compensation temperatures.

In order to complete our analysis of the magnetization, let us recall that for non-zero values of λ , the most interesting thermal variations of the magnetization appears in the ferrimagnetic case (i.e, $\alpha < 0$) in the region where compensation effects take place. To illustrate this original behavior, we have depicted in Fig. 7 the magnetization curves exhibiting one (the red curve) and two compensation temperatures (the green curve). It follows from the previous discussion that the system with pure three-site

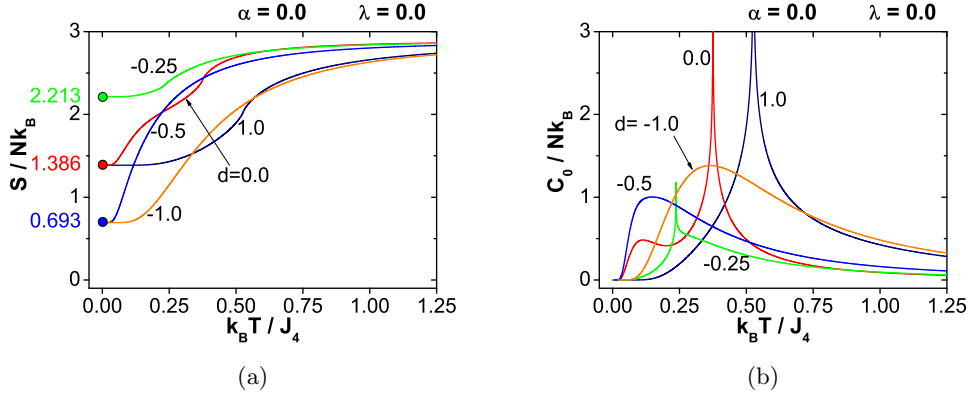


Figure 8: (a) - Thermal dependencies of reduced entropy of the decorated mixed-spin Ising system for $\alpha = \lambda = 0.0$ and for several typical values of d . (b) - Thermal dependencies of reduced specific heat of the decorated mixed-spin Ising system for $\alpha = \lambda = 0.0$ and the same values of d as in case (a).

four-spin interaction will necessarily exhibit finite values of entropy in the ground state. This interesting phenomenon is investigated in Fig. 8a, where we have depicted the temperature dependencies of entropy for $\alpha = \lambda = 0$ and several values of d corresponding to Figs. 6a and 6b. The results shown in this figure prove that the ground-state entropy

of the system may take only three different values depending on the value of d , namely,

$$\begin{aligned}
S_0 &= Nk_B \ln 2 \approx 0.693Nk_B & \text{for } d < -0.25 \\
S_0 &= 2Nk_B \ln 2 \approx 1.386Nk_B & \text{for } d > -0.25. \\
S_0 &\approx 2.213Nk_B & \text{for } d = -0.25.
\end{aligned}
\tag{23}$$

Here one should notice that the value of $S_0 \approx 0.693Nk_B$ originates solely from the contribution of the A sublattice, while the second non zero value of $S_0 \approx 1.386Nk_B$ represents exclusive contribution of the B sublattice. Of course, these two values correspond to ground-state spin configurations described in detail in the Subsection 4.1. On the other hand, the value of entropy for $d = -0.25$ consists apparently from two parts, i.e., $S_0 = S_{0B} + S_{0A} = 2.213Nk_B$, where the major contribution comes from the B sublattice where all three spin states $S_i^z = 0, \pm 1$ are randomly occupied at $T = 0$ (see green curve in Fig. 8a). The small supplementary value S_{0A} represents the contribution of the A sublattice which is also slightly disordered at $T = 0$ since the sublattice magnetization m_A does not reach its saturated value (see green curve in Fig. 6a). Here we should also mention that the results for ground state entropy in case of $\lambda \neq 0.0$, that is when next-nearest interaction is present, revealed just two values of entropy at $T = 0$, from which one of them equals 0 (see also ground state analysis in Subsection 4.1). Comparing different entropy behavior in ground states for pure three-site four-spin interaction and those with additional bilinear interactions (J, J') one can see a significant signature of three-site four-spin interaction in pushing the system to the unconventional partially ordered states.

Finally, we have calculated the temperature dependencies of the magnetic specific heat and the results obtained for a special case of $\alpha = 0, \lambda = 0$ are presented in Fig. 8b. As one can see from the figure, the curves for $d = 1.0, 0.0$ and -0.25 exhibit at critical point a logarithmic singularity similarly as the usual spin-1/2 Ising model on a square lattice. Similarly, for strong negative values of d one observes the expected behavior for paramagnetic systems. One should emphasize here that despite of non-zero ground-state entropy (cf. Fig. 8a), the specific heat goes always to zero for $T \rightarrow 0$, so that the Third law of thermodynamics is perfectly satisfied.

5. Conclusion

In this work we have concentrated on clarifying the influence of three-site four-spin interactions on magnetic properties of a mixed-spin Ising model on the decorated square lattice including also the pair exchange interaction and crystal-field contributions. Applying the generalized decoration-iteration transformation, we have exactly obtained all relevant physical quantities of the model, including the ground-state and finite-temperature phase diagrams. The numerical results obtained in this work clearly illustrate the principal influence of higher-order spin interactions on all relevant physical quantities. The most original behavior has been observed in the case with pure three-site four spin interactions, where we have confirmed that unlike of four-site four-spin interactions (see [11]-[14]) the three-site four-spin interactions may initiate the appearance of a partial long-range order. Moreover, due to the very strong frustrations in the system one observes a non-zero entropy at $T = 0$ over a wide range of parameters.

In general, it is necessary to emphasize that the multi-spin interactions have as a rule very different symmetries in comparison with those of the pair (bilinear) interaction terms and, of course, these new symmetries basically determine the behavior of the system. It is well known that the theoretical investigation of the systems with many-body interactions is extraordinarily complicated task, thus the absolute majority of the papers in diverse research fields treat only the systems with two-body (pair-wise) interactions. One should, however, notice that various versions of Ising and Heisenberg models represent rare exceptions that straightforwardly enable to account for many different forms of multi-spin (i.e. many-body) interactions. For that reason the localized-spin models represent an excellent basis for deep understanding of various many-body interactions going beyond the standard pair-wise picture. We hope that the present study will may initiate a wider interest in investigation of magnetic systems with multi-spin interactions.

Appendix

The coefficients A_0 , A_1 , A_2 are respectively given by

$$A_0 = \frac{1}{2} \left[G\left(J, \frac{J_4}{4}\right) + G\left(0, -\frac{J_4}{4}\right) \right]$$

$$A_1 = F\left(J, \frac{J}{4}\right)$$

$$A_2 = \frac{1}{2} \left[G\left(J, \frac{J_4}{4}\right) - G\left(0, -\frac{J_4}{4}\right) \right]$$

where

$$G(x, y) = \frac{2 \cosh(\beta x)}{2 \cosh(\beta x) + \exp(-\beta D - \beta y)}$$

$$F(x, y) = \frac{2 \sinh(\beta x)}{2 \cosh(\beta x) + \exp(-\beta D - \beta y)}$$

References

- [1] F. Y. Wu, Phys. Rev. B 4 (1971) 2312.
- [2] L. P. Kadanoff and F. J. Wegner, Phys. Rev. B 4 (1971) 3989.
- [3] F. Y. Wu, Phys. Lett. A 38 (1972) 77.
- [4] R. V. Ditzian, Phys. Lett. A 42 (1972) 67.
- [5] M. Suzuki, Phys. Rev. Lett. 28 (1972) 507.
- [6] T. Horiguchi, Physica A 130 (1985) 194.
- [7] T. Horiguchi, L.L. Goncalves, Physica A 133 (1985) 460.
- [8] T. Morita, T. Horiguchi, Physica A 136 (1986) 99.
- [9] F. Wang, M. Suzuki, Physica A 230 (1996) 639.
- [10] A. Lipowski, Physica A 248 (1998) 207.
- [11] S. Lacková, M. Jaščur, Phys. Rev. E 64 (2001) 036 126.
- [12] S. Lacková, M. Jaščur, Czech. J. Phys. 52 (2001) A33.
- [13] S. Lacková, M. Jaščur, Physica A 326 (2003) 189.
- [14] S. Lacková, M. Jaščur, T. Horiguchi, Physica A 339 (2004) 416.
- [15] M. Jaščur, V. Štubňa, K. Szalowski, T. Balcerzak, Acta Phys. Polonica 126 (2014) 48.
- [16] J. Oitmaa, R.W. Gibberd, J. Phys. C 6 (1973) 2077.
- [17] H.P. Griffiths, D.W. Wood, J. Phys. C 7 (1974) L54.
- [18] H.P. Griffiths, D.W. Wood, J. Phys. C 7 (1974) 4021.
- [19] M. Nauenberg, B. Nienhuis, Phys. Rev. Lett. 33 (1974) 944.
- [20] J.M.J. van Leeuwen, Phys. Rev. Lett. 34 (1975) 1056.
- [21] M.P. Nightingale, Phys. Lett. 59A (1977) 468-
- [22] F. Lee, H.H. Chen, F.Y. Wu, Phys. Rev. B 40 (1989) 4871.
- [23] D.F. Styer, M.K. Phani, J.L. Lebowitz, Phys. Rev. B 34 (1986) 3361.
- [24] K.K. Chin, D.P. Landau, Phys. Rev. B 36 (1987) 275.
- [25] J.R. Heringa, H.W.J. BlWote, A. Hoogland, Phys. Rev. Lett. 63 (1989) 1546.
- [26] G.-M. Zhang, C.-Z. Yang, Phys. Rev. B 48 (1993) 9487.
- [27] C.L. Wang, Z.K. Qin, D.L. Lin, J. Magn. Magn. Mater. 88 (1990) 87.
- [28] T. Kaneyoshi, T. Aoyama, J. Magn. Magn. Mater. 96 (1991) 67.
- [29] K.G. Chakraborty, J. Magn. Magn. Mater. 114 (1992) 155.
- [30] S. Lacková, M. Jaščur, J. Magn. Magn. Mater. 217 (2000) 216.
- [31] M. Grimsditch, P. Loubeyre and A. Polian, Phys. Rev. B 33 (1986) 7192.
- [32] M. Roger, J. H. Hetherington and J. M. Delrieu, Rev. Mod. Phys. 55 (1983) 1.
- [33] H. L. Scott, Phys. Rev. A 37 (1988) 263.
- [34] Z. Onyszkiewicz, Phys. Lett. 68 A (1978) 113.
- [35] J. A. Barker, Phys. Rev. Lett. 57 (1986) 230.
- [36] W. Chunlei, Q. Zikai and Z. Jingbo, Ferroelectrics 77 (1988) 21.
- [37] C.L. Wang, Z.K. Qin, D.L. Lin, Phys. Rev. B 40 (1980) 680.
- [38] C.L. Wang, Z.K. Qin, D.L. Lin, Solid State Commun. 71 (1989) 45.
- [39] P.R. Silva, B.V. Costa, R.L. Moreira, Polymer 34 (1993) 3107.
- [40] S. Brehmer, H.-J. Mikeska, M. MXuller, Phys. Rev. B 60 (1999) 329.
- [41] M. Matsuda, K. Katsumata, Phys. Rev. B 62 (2000) 8903.
- [42] M. Matsuda, K. Katsumata, R.S. Eccleston, S. Brehmer, H.-J. Mikeska, J. Appl. Phys. 87 (2000) 6271.
- [43] K.P. Schmidt, C. Knetter, G.S. Uhrig, Europhys. Lett. 56 (2001) 877.
- [44] T.S. Nunner, P. Brune, T. Kopp, M. Windt, M. GrXuninger, Acta Phys. Pol. B 34 (2003) 1545.
- [45] Y. Honda, Y. Kuramoto, T. Watanabe, Phys. Rev. B 47 (1993) 11329.
- [46] R. Coldea, S.M. Hayden, G. Aeppli, T.G. Perring, C.D. Frost, T.E. Mason, S.-W. Cheong, Z. Fisk, Phys. Rev. Lett. 86 (2001) 5377.
- [47] T. Iwashita and N. Uryu, J. Phys. C: Solid State Phys. 17 (1984) 855.
- [48] T. Iwashita and N. Uryu, J. Phys. C: Solid State Phys. 21 (1988) 4783.
- [49] T. Iwashita and N. Uryu, Phys. Lett. A 125 (1987) 5.
- [50] T. Iwashita and N. Uryu, Phys. Lett. A 155 (1991) 241.
- [51] U. Köbler, R. Mueller, L. Smardz, D. Maier, K. Fischer, B. Olefs, W. Zinn, Z. Phys. B 100 (1996) 497.
- [52] E. Müller-Hartmann, U. Köbler, L. Smardz, J. Magn. Magn. Mater. 173 (1997) 133.
- [53] U. Köbler, R.M. Mueller, W. Schnelle, K. Fischer, J. Magn. Magn. Mater. 188 (1998) 333.

- [54] U. Köbler, A. Hoser, M. Kawakami, T. Chatterji, J. Rebizant, J. Magn. Mater. 205 (1999) 343.
- [55] I. Syozi, Prog. Theor. Phys. 6 (1952) 341.
- [56] I. Syozi, in *Phase Transition and Critical Phenomena*, edited by C. Domb and M.S. Green Academic Press, New York, 1972.
- [57] M. Fisher, Phys. Rev. 113 (1959) 969
- [58] L. Onsager, Phys.Rev. 65 (1944) 117.
- [59] H. B. Callen, Phys. Lett. 4 (1963) 161.
- [60] M. Suzuki, Phys. Lett. 19 (1965) 267.
- [61] R. Honmura and T. Kaneyoshi, J. Phys. C 12 (1979) 3979.